

INCORPORATION OF FE-F6 BLOCKS INTO LAMINAR HYDROXIDES OF FE, NI: EXPLORING ON THE WATER OXIDATION REACTION

**Ariel Guzmán Vargas^{*1}, María de Jesús Martínez Ortiz¹,
Carlos Felipe Mendoza², Enrique Lima³**

¹Instituto Politécnico Nacional-ESIQIE-SEPI-DIQI-LiMpCa-QuF, UPALM, Zacatenco, CDMX, 07738, CDMX, Mexico.

²Instituto Politécnico Nacional –CIEMAD- D. de Biociencias e Ingeniería, CDMX 07340, Mexico.

³Universidad Nacional Autónoma de México- LaFReS, IIM, Circuito Exterior s/n, Cd. Universitaria, Coyoacán, CDMX 04510, Mexico.

aguzmanv@ipn.mx

Guzmán Vargas, A., Martínez Ortiz, M. J., Felipe Mendoza, C., & Lima, E. (2023). Incorporation of Fe-F6 blocks into laminar hydroxides of Fe, Ni: Exploring on the water oxidation reaction. In E. San Martín-Martínez (Ed.). *Research advances in nanosciences, micro and nanotechnologies. Volume IV* (pp. 177-190). Barcelona, Spain: Omniascience.

Abstract

Nanostructured materials offer important characteristics to be applied in different fields of research, for example, in renewable and clean energy production processes in electrolyzers for the generation of hydrogen from water, reaction known as water splitting or oxidation. In the present work, the studies carried out with Ni, Fe layered double hydroxides (LDH) are reported, modified with the introduction of FeF_6 blocks containing fluoride (Fe-F) with 10 and 20 %w, in the brucite-type layers, which will partially occupy structural positions of the Fe-hydroxyl groups (Fe-OH). The method of synthesis used was coprecipitation at low saturation with the aim to obtain nanocrystals. The incorporation of Fe in the structure of nanomaterials was made in its Fe^{3+} form as M^{3+} cation, and nickel as M^{2+} cation, respectively, maintaining a $\text{M}^{2+}/\text{M}^{3+} = 3$ molar ratio. The physicochemical properties of the materials were characterized by different techniques such as: XRD, ^{19}F -NMR, IR, TGA/DSC, nitrogen physisorption. The results revealed well-ordered materials, structural modifications and changes in the thermal and adsorption properties, as a consequence of the incorporation of Fe-F_6 species in the brucite-type sheets.

The electrocatalytic properties of the materials as electrodes, were evaluated in the oxygen evolution reaction (OER) in an alkaline medium, determining the parameters such as: overpotential, Tafel slope, activation energy, electrochemically active surface area (ECSA) and stability. All samples exhibited responses on the OER, the fluorinated samples showed an overpotential of 1.16 -1.22 V and a Tafel slope of 285 - 331 mV/decade.

Keywords: Fluorinated LDH; OER; Water Oxidation; Electrocatalysis.

1. Introduction

Two dimensional nanostructured materials as Layered Multihydroxides (LMH or LDH) are formed by brucite-type layer with positive charge which is compensated by anionic species in the interlaminar or interlayer region. Their molecular formula is $[M^{II}_{1-x}M^{III}_x(OH)_2]^{x+}(A^n)_{x/n} \cdot mH_2O$, and their composition should include a wide variety of divalent metal ions octahedrally coordinated to hydroxyl groups in the brucite-type layers ($M^{II}=Mg^{2+}, Co^{2+}, Cu^{2+}, Ni^{2+}$ or Zn^{2+}), these cations should be isomorphically replaced by trivalent cations as ($M^{III}=Al^{3+}, Fe^{3+}, Mn^{3+}, Cr^{3+}$ or Ga^{3+}) [1, 2]. In this context, the basicity attributed to the OH^- can be tailored by the presence of electronegative species. For this purpose, the first reports showed the impregnation method to introduce fluorinated species on the layer's surface in order to increase the basicity properties [3]. Thus, Lima *et al.* reported the first LDH material incorporating F as $(AlF_6)^{3-}$ blocks in the brucite-type layer, replacing $Al(OH)_6^{3-}$ by $(AlF_6)^{3-}$ blocks, obtaining a new class of material with different properties as acid-base [4]. With this aim, as an alternative to RuO_2 and IrO_2 materials, NiFe LDHs have been presented good response on the OER [5 – 8], which is the rate determining step (RDS) on the water splitting or oxidation to produce hydrogen from industrial electrolyzers, as alternative source of green and renewable energy from non-fossil origin in the context of the environmental crisis and the energy transition [9 – 11]. In this work, we reported the preparation of LDH containing F species, incorporating $(FeF_6)^{3-}$ instead of $Fe(OH)_6^{3-}$ blocks in the layer or sheet. As first approach, the solids were evaluated on OER process to prove some electrocatalytic aspects of this kind of nanomaterials.

2. Experimental

2.1. Synthesis and electrode preparation

The NiFe LDHs were prepared by coprecipitation method using as source of fluorine and precursors of metal cations were $Ni(NO_3)_2 \cdot 6H_2O$, and $Fe(NO_3)_3 \cdot 9H_2O$; two samples with 10 and 20 %w of Fe-F, and one sample without F, all solids with a Ni/Fe = 3 molar ratio, the equipment used to perform the synthesis of the materials was a pH STAT Titrino (Metrohm). The work electrodes were obtained by mixing the prepared LDHs in a solution of nafion and ethanol, this suspension was sonicated for 30 min, then, around 80 μ L were deposited on a

piece of glassy carbon to form a uniform film and dried at room temperature. The samples were labeled as NiFe-10F, NiFe-20F and NiFe.

2.2. *Characterization and Electrochemical Tests*

Powder X-ray diffraction analysis (PXRD) were carried out in an X'Pert PRO with a $\text{CuK}\alpha=1.5406 \text{ \AA}$ (45 kV and 40 mA) in the interval of 5 to 80 (2θ). The diffractograms were acquired with the step of 0.02 and 0.4 s for each point. FTIR spectra were obtained using a Frontier Perkin Elmer spectrometer with an ATR accessory, acquisition was performed between 500 and 4000 cm^{-1} , with a resolution of 2 cm^{-1} . The ^{19}F MAS NMR spectra were measured in an Avance 300 Bruker instrument operating the spectrometer at 376.3 MHz, using $\pi/2$ pulses of 6 ms with a recycle delay of 1 s; ^{19}F chemical shifts were referenced to those of CFCl_3 at 0 ppm. Thermal analyses were carried out employing a STA 6000 TGA/DSC Perkin Elmer apparatus in the range of temperature between 25 to 900 $^\circ\text{C}$, in a N_2 atmosphere as carrier gas. Textural properties were measured in Autosorb iQ Station Quantachrome Instruments. The solids were previously out gassed in N_2 at 160 $^\circ\text{C}$ for 2 h, adsorption-desorption isotherms were collected in the range of 0.015 a 0.99 for P/Po.

The supported films were then used as working electrode in a three-electrode one compartment standard electrochemical cell. Graphite and Hg/HgO NaOH 0.1 M (0.164 V vs RHE) electrodes were employed as counter and reference electrode, respectively. Electrochemical analyses were carried out at room temperature in a multichannel PGstat302N potentiostat-galvanostat (Autolab). Rotating Disk Electrode method was employed for electrocatalytic evaluation at 1600 rpm, in the window of 0 V to 1.6 V at scan of 10 mV/s. For all set of experiments, linear voltammetry was reported with compensated cell resistance (iR). The Reversible Hydrogen Electrode (RHE) scale was calculated based on the formula: $\text{VRHE}=\text{VSCE}+\text{VSCE}(\text{vs NHE})+(0.059*\text{pH})$.

3. Results and Discussion

3.1. *Structural Characterization*

Typical LDH crystalline structure was confirmed by XRD patterns for samples containing a mixture of Fe-F and Fe-OH groups and the sample without Fe-F species (Figure 1). For the three samples, the patterns show LDH phase with the usual hexagonal lattices and R3m rhombohedral symmetry (JCPDS 22-0700) [12, 13].

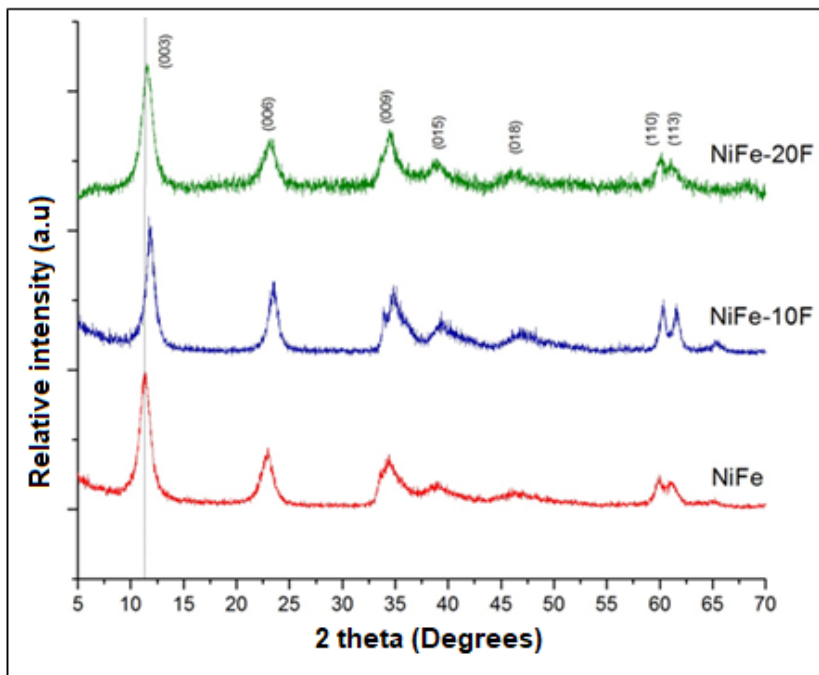


Figure 1. XRD patterns of layered materials with FeF₆ incorporated blocks, the solid NiFe is without flour.

All samples exhibit well-defined peaks for the (003), (006) and (009) planes, related to the interlayer space. Furthermore, it should be remarked that the peaks for sample NiFe-10F sample are broader compared to the other two samples.

Moreover, the peak in the plane (003) was slightly shifted for the samples containing F, this is associated to the strong interaction between fluorine, the cations in the brucite-like layers and the anions in the interlayer space [4]. This is also in accord to the values of c and d_{003} parameters as shown in the table 1, both parameters decrease when Fe-F species are present, while the cell parameter a , related to the distance between adjacent cations in the layer, is similar for all samples.

Table 1. Cell parameters of LDH samples.

Sample	d_{003} (Å)	d_{110} (Å)	a (Å)	c (Å)
NiFe	7.82	1.54	3.09	23.47
NiFe-10F	7.56	1.53	3.07	22.67
NiFe-20F	7.69	1.54	3.08	23.08

IR spectra are exhibited in Figure 2. OH⁻ groups from water in the interlayer region and on the sheets are described by the presence of band around 3000-3600 cm⁻¹, specially, in the samples fluorinated this stretching vibration band is broader and more intense due to the dipolar moment indicating that these samples are more hydrated. The band at 1630 cm⁻¹ is attributed to the deformation plane of water. C-O asymmetric stretching vibration of CO₃²⁻ is observed at 1360 cm⁻¹. In the range between 1000 to 500 cm⁻¹ the bands are associated to M-O, M-O-M and O-M-O bonds in the brucite-like layers, typical bands of these kind of materials. For these samples, they correspond to the Ni-oxygen and Fe-oxygen lattice vibrations [14].

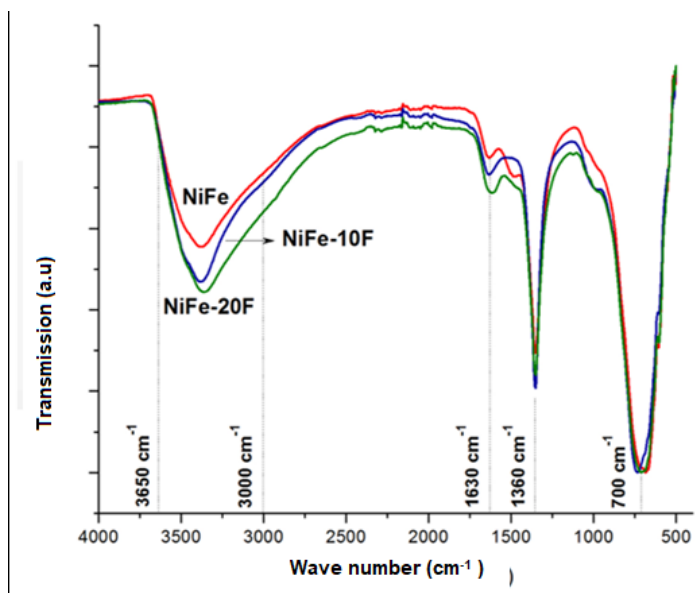


Figure 2. FTIR spectra of LDH solids with and without flour.

In order to verify the incorporation of Flour (Fe-F₆ blocks) in the brucite type layer, substituting partially OH⁻ groups (Fe-OH), ¹⁹F NMR studies were carried out. The spectra of ¹⁹F nuclei are shown in Figure 3 for the samples. Three main signals were observed, a shoulder around -147, at -133 and -93 ppm. The peak at -147 ppm is associated to (FeF₆)³⁻ species as it was previously reported [15, 16]. In addition, other resonances a lower field (-133 and -93 ppm) suggest the existence of octahedral blocks type (FeF_{6-x}(OH)_x)³⁻ which means that the (FeF₆)³⁻ blocks are randomly mixed with Fe(OH)₆³⁻ or (Ni(OH)₆)⁴⁻ blocks in the layer sheet. Thus, the main signal at -147 ppm point out the presence of domains rich in fluorinated blocks combined with zones rich in OH⁻.

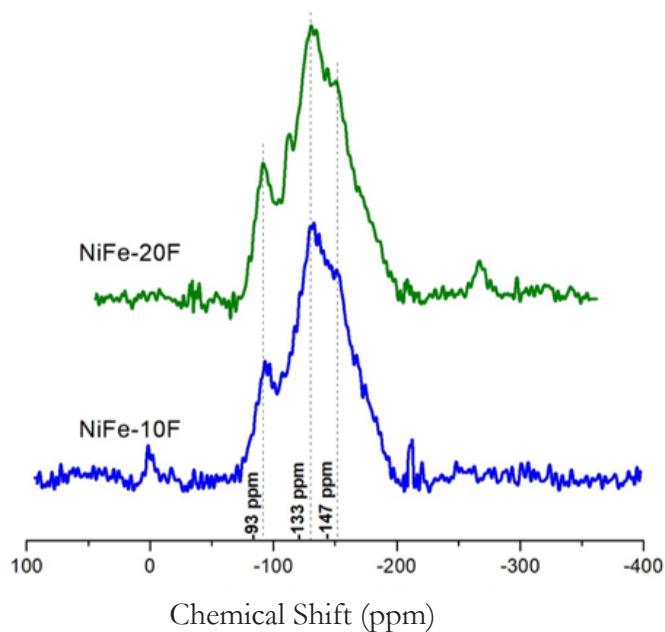


Figure 3. ^{19}F NMR spectra of NiFe-20F and NiFe-10F.

3.2. Thermal Analysis, morphology, and textural properties

Profiles of thermal analyses are shown in Figure 4, three zones of mass loss are clearly observed. The first around 100 °C, is associated to desorption of water on the surface. The second between 170 °C and 305 °C is attributed to the loss of water in the interlayer space and dehydroxylation. It is observed that the samples containing F show a fast loss of weigh, considering these materials

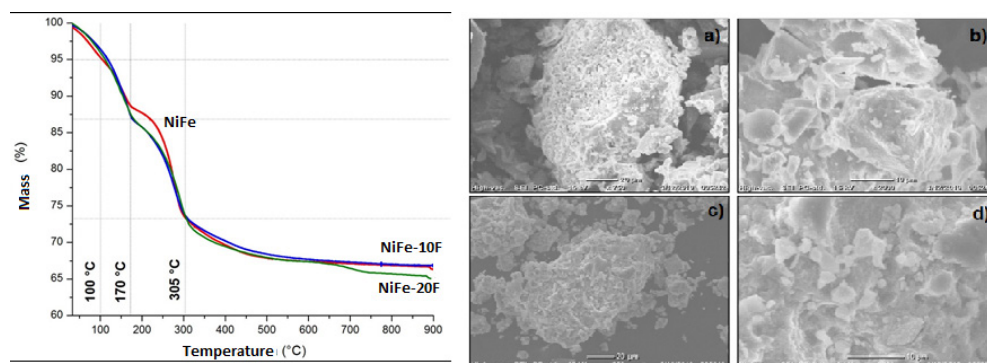


Figure 4. Thermal profiles of NiFe LDH and SEM images of a) and b) NiFe-10F, c) and d) NiFe-20F.

are more hydrated as above discussed. Besides, in the last zone up to 305 °C, the process of decarbonation takes place at the same time that the dihydroxylation is completed [17]. In general, all the samples exhibited the same percent of weight loss. Finally, the total mass loss was similar for all samples, the presence of flour has not important influence on the thermal stability at higher temperatur

Figure 4 a) to d) shows SEM images of the F containing samples, the form observed was flakes or irregular plaques, typical for layered materials, with sizes between 10-100 μm , there is not important influence of flour presence on the morphology.

Adsorption-desorption isotherms are shown in Figure 5; the profile of all samples corresponds to type IV, showing H2 type hysteresis loop according to IUPAC classification, typical for mesoporous materials showing desorption pore blocking effects [18]. This last phenomenon was more marked on the flour samples; it can be associated with the strong interaction of fluorinated species and

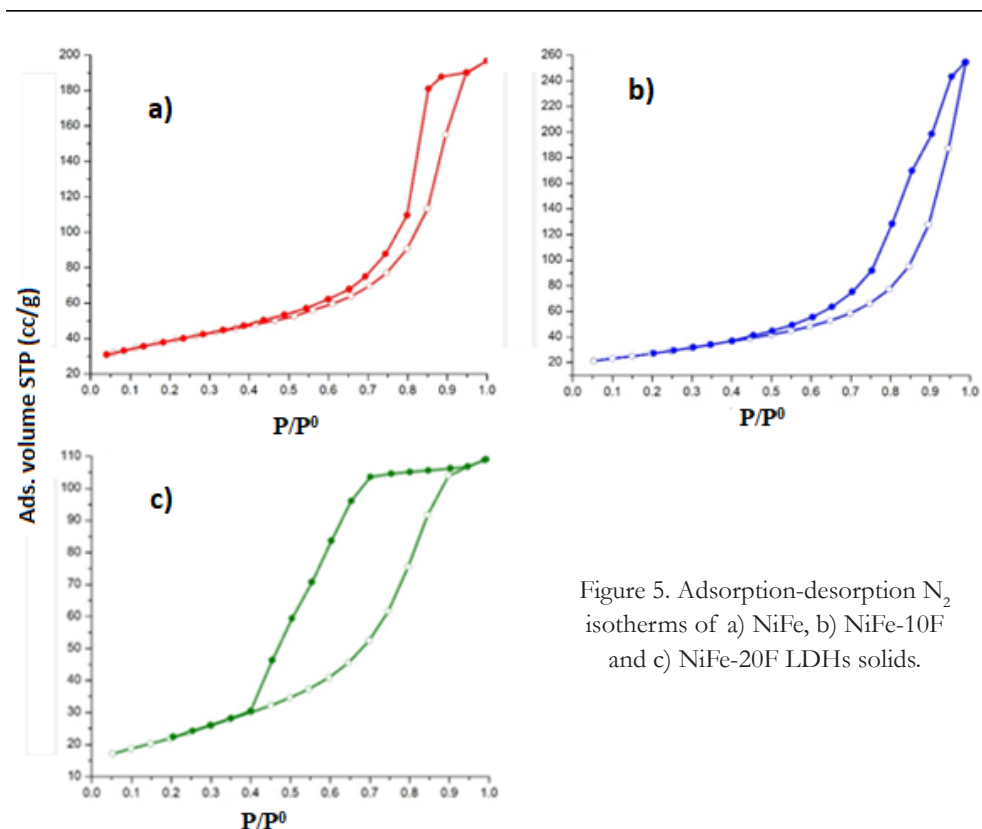


Figure 5. Adsorption-desorption N_2 isotherms of a) NiFe, b) NiFe-10F and c) NiFe-20F LDHs solids.

the higher degree of hydration, as reported in TGA studies. The profiles can also be associated with different sizes of pores.

Regarding the shape of the hysteresis loops, for the sample in red (see Figure 5), the pores are of similar sizes, causing slight pore blockage during desorption. In contrast, more significant pore blockage is appreciated in the green isotherm. On the other hand, the null pore blockage is evident in the blue isotherm due to the gradual filling and emptying of the pores.

For the results of a specific surface, the solid without F exhibited the largest values, and the samples with F showed a lower surface. This agrees with adsorption-desorption isotherms; the presence of F can block some part of the porous structure provoking the decrease of the area BET, volume and radius of the pore, as it is reported in Table 2.

Table 2. Textural properties of LDH samples.

Sample	ABET (m ² /g)	Pore Vol.* (cm ³ /g)	Pore Radius Å
LDH NiFe SF	132.00	0.263	61.76
LDH NiFe 10 % F	43.56	0.394	48.65
LDH NiFe 20 % F	80.25	0.169	17.15

3.3. First Approach: Exploring the electrocatalytic properties on the water oxidation reaction (OER)

This kind of materials have been reported as electrocatalysts for the water oxidation reaction, in some studies Ni was founded that it acts as catalytic center protected by Fe, taking into account the adsorption of OH⁻ as principal step [6, 19]. From this, we reported as first approach to examine some properties of this kind of materials, the performance on OER or water oxidation.

The overpotential (η) is a parameter to measure the catalytic activity, it is reported to reach current density (j) of 10 mA/. Figure 6 shows the profiles for the samples. Clearly, a positive effect due to the Fe-F species is observed. The best performance was for NiFe-20F with the lowest value around 868 mV. This behavior can be attributed to the formation of more catalytic sites when F is present and it is was corroborated determining the electrocatalytic surface area (ECSA) where the sample NiFe-20F showed a value of 0.530 cm², while the sample without F was 0.47 cm².

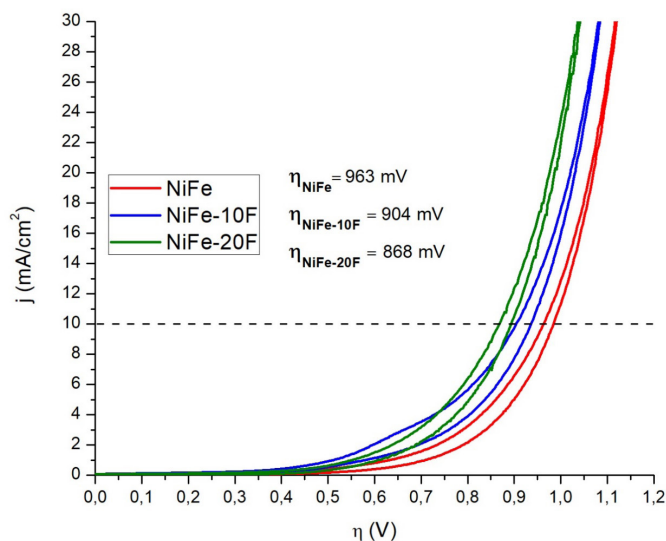


Figure 6. Overpotential on the OER process of LDH samples at $j=10 \text{ mA/cm}^2$.

NiFe fluorinated LDHs revealed overpotential values around 300 mV. Some aspects could be considered to explain this behavior. It is well known the electronegativity associated to the presence of fluorine, and the OER mechanism is mainly associated to the OH^- adsorption, although, it is possible the strong adsorption of the OH^- . Species limiting the electron transfer due to the force of the electronegativity. To solve this inhibition, the presence of another kind of catalytic site i.e Co or improve the distribution of Fe-F blocks so as not creates richest zones of these species. Testing these kind of materials in reactions where strong electronegativity and basicity plays an important role as in some processes i.e. C-C bond formation [20].

4. Conclusions

Nanostructured Layered hydroxides of NiFe (NiFe-LDH) were obtained incorporating Fe-F6 blocks, which partially substituted to the Fe-OH or Ni-OH blocks in the brucite-type sheets using the coprecipitation method. The main goal of this study was achieved in order to demonstrate the introduction of iron fluorinated species in the layers to obtain a new kind of material. This was demonstrated by different techniques, from the XRD results typical diffraction patterns of layered hydroxide materials were obtained and corroborated with the

values of a and d_{003} parameters. The presence of fluorinated species was confirmed by ^{19}F NMR showing characteristic bands associated to fluor interactions. Adsorption-desorption Isotherms were of mesoporous solids, a strong adsorption was observed due to the Fe-F₆ blocks. As first approach, the electrocatalytic properties were evaluated in the OER process in alkaline media.

Funding

This study was partially supported by the Projects SIP-IPN 20211169 and 20220802.

References

1. Cavani, F., Trifirò, F., & Vaccari, A. (1991). Hydrotalcite-type anionic clays: Preparation, properties and applications. *Catalysis Today*, 11, 173-301.
[https://doi.org/10.1016/0920-5861\(91\)80068-K](https://doi.org/10.1016/0920-5861(91)80068-K)
2. Shao, M., Zhang, ., Li, Z., Wei, M., Evans, D. G., & Duan, X. (2015). Layered double hydroxides toward electrochemical energy storage and conversion: design, synthesis and applications. *Chemical Communications*, 51, 15880-15893.
<https://doi.org/10.1039/C5CC07296D>
3. Choudary, B. M., Kantam, M. L., Neeraja, V., Rao, K. K., Figueras, F., & Delmotte, L. (2001). Layered double hydroxide fluoride: a novel solid base catalyst for C–C bond formation. *Green Chemistry*, 5, 257-260.
<https://doi.org/10.1039/b107124f>
4. Lima, E., Martínez-Ortiz, M. J., Gutiérrez Reyes, R. I., & Vera, M. (2012). Fluorinated Hydrotalcites: The Addition of Highly Electronegative Species in Layered Double Hydroxides To Tune Basicity. *Inorganic Chemistry*, 51(14), 7774-7781.
<https://doi.org/10.1021/ic300799e>
5. Gong, M., & Dai, H. (2015). A mini review of NiFe-based materials as highly active oxygen evolution reaction electrocatalysts. *Nano Research*, 8, 23-29.
<https://doi.org/10.1007/s12274-014-0591-z>
6. Carrasco, J. A., Romero, J., Varela, M., Hauke, F., Abellán, G., Hirsch, A. *et al.* (2016). Alkoxide-intercalated NiFe-layered double hydroxides magnetic nanosheets as efficient water oxidation electrocatalysts. *Inorganic Chemistry, Frontiers*, 3, 478-487.
<https://doi.org/10.1039/C6QI00009F>
7. Guzmán-Vargas, A., Vazquez-Samperio, J., Oliver-Tolentino, M. A., Ramos-Sánchez, G., Flores-Moreno, J. L., & Reguera, E. (2017). Influence on the Electrocatalytic Water Oxidation of M²⁺/M³⁺ Cation Arrangement in NiFe LDH: Experimental and Theoretical DFT Evidences. *Electrocatalysis*, 8, 383-391.
<https://doi.org/10.1007/s12678-017-0383-9>
8. Lu, Z., Xu, W., Zhu, W., Yang, Q., Lei, X., Liu, J. *et al.* (2014). Three-dimensional NiFe layered double hydroxide film for high-efficiency oxygen evolution reaction. *Chemical Communications*, 49, 6479-6482.
<https://doi.org/10.1039/C4CC01625D>
9. Long, X., Li, J., Xiao, S., Yan, K., Wang, Z., Chen, H. *et al.* (2014). A strongly coupled graphene and FeNi double hydroxide hybrid as an excellent electrocatalyst for the oxygen evolution reaction. *Angewandte Chemie*, 126, 7714-7718.
<https://doi.org/10.1002/ange.201402822>

10. Dresp, S., Luo, F., Schmack, R., Kuhl, S., Gliech, M., & Strasser, P. (2016). An efficient bifunctional two-component catalyst for oxygen reduction and oxygen evolution in reversible fuel cells, electrolyzers and rechargeable air electrodes. *Energy & Environmental Science*, 9, 2020-2024.
<https://doi.org/10.1002/ange.201402822>
11. Long, X., Wang, Z., Xiao, S., An, Y., & Yang, S. (2016). Transition metal based layered double hydroxides tailored for energy conversion and storage. *Materials Today*, 19, 213-226.
<https://doi.org/10.1016/j.mattod.2015.10.006>
12. Di Cosimo, J. I., Díez, V. K., Xu, M., Iglesia, E., Apesteguía, C. R. (1998). Apesteguía, Structure and Surface and Catalytic Properties of Mg-Al Basic Oxides. *Journal of Catalysis*, 178(2), 499-510.
<https://doi.org/10.1006/jcat.1998.2161>
13. Shanon, R. D. (1976). Revised Effective Ionic Radii and Systematic Studies of Interatomic Distances in Halides and Chalcogenides. *Acta Cryst.*, A32, 751-767.
<https://doi.org/10.1107/S0567739476001551>
14. Liao, F., Yang, G., Cheng, Q., Mao, L., Zhao, X., & Chen, L. (2022). Rational design and facile synthesis of Ni-Co-Fe ternary LDH porous sheets for high-performance aqueous asymmetric supercapacitor. *Electrochimica Acta*, 428, 140939.
<https://doi.org/10.1107/S0567739476001551>
15. Asseid, F. M., Duke, C. V. A., Miller, J. M. (1990). A ¹⁹F magic angle spinning nuclear magnetic resonance and infrared analysis of the adsorption of alkali metal fluorides onto montmorillonite clay. *Canadian Journal of Chemistry*, 68(8), 1420.
<https://doi.org/10.1139/v90-217>
16. Scholz, G., Krahl, T., Ahrens, M., Martineau, C., Buzaré, J. Y., Jäger, C. *et al.* (2011). ¹¹⁵In and ¹⁹F MAS NMR study of (NH₄)₃InF₆ phases. *Journal of Fluorine Chemistry*, 132(4), 244-249.
<https://doi.org/10.1139/v90-217>
17. Magri, V. R., Duarte, A., Perotti, G. F., & Constantino, V. R. L. (2019). Investigation of Thermal Behavior of Layered Double Hydroxides Intercalated with Carboxymethylcellulose Aiming Bio-Carbon Based Nanocomposites. *ChemEngineering*, 3(2) 55.
<https://doi.org/10.1139/v90-217>
18. Cychosz, K. A., & Thommes, M. (2018). Progress in the physisorption characterization of nanoporous gas storage materials. *Engineering*, 4(4), 559-566.
<https://doi.org/10.1016/j.eng.2018.06.001>

19. Abellán, G., Coronado, E., Martí-Gastaldo, C., Waerenborgh, J., & Ribera, A. (2013). Interplay between chemical composition and cation ordering in the magnetism of Ni/Fe layered double hydroxides. *Inorganic Chemistry*, 52(17), 10147-10157.
<https://doi.org/10.1016/j.eng.2018.06.001>
20. Tichit, D., & Álvarez, M. G. (2022). Layered Double Hydroxide/Nanocarbon Composites as Heterogeneous Catalysts: A Review. *ChemEngineering*, 6(4), 45.
<https://doi.org/10.1016/j.eng.2018.06.001>